

Six-moment representation of multiple aerosol populations in a sub-hemispheric chemical transformation model

D. L. Wright, R. McGraw, C. M. Benkovitz, and S. E. Schwartz

Environmental Chemistry Division, Department of Applied Science, Brookhaven National Laboratory, Upton, New York

Abstract. This letter describes the first application of the Quadrature Method of Moments (QMOM) [McGraw, 1997] in a 3-D chemical transformation and transport model. The QMOM simultaneously tracks an arbitrary (even) number of moments of a particle size distribution directly in space and time without the need for explicitly representing the distribution itself. The host 3-D model, the Global Chemistry Model driven by Observation-derived meteorological data (GChM-O), has been previously described [Benkovitz *et al.*, 1994]. The present implementation evolves the six lowest-order radial moments for each of several externally-mixed aerosol populations. From these moments we report modeled geographic distributions of several aerosol properties, including a shortwave radiative forcing obtained using the Multiple Isomomental Distribution Aerosol Surrogate (MIDAS) technique [Wright, 2000]. These results demonstrate the capabilities of these moment-based techniques to simultaneously represent aerosol nucleation, condensation, coagulation, dry deposition, wet removal, cloud activation, and transport processes in a large scale model, and to yield aerosol optical properties and radiative influence from the modeled aerosol.

1. Introduction

There is a growing need for efficient representation of aerosol microphysical processes in atmospheric chemistry and transport models, especially regarding the radiative effects of natural and anthropogenic aerosols and their impact on climate [Haywood *et al.*, 1999; Bergstrom and Russell, 1999]. Most current models explicitly represent the aerosol size distribution with either discrete bins (the sectional approach) or with assumed functional forms for various modes in the distribution (the modal approach). These are standard modeling schemes well-investigated in the literature. More recently there has been exploration of representing aerosols by the moments of the size distribution alone, without the necessity of tracking the size distribution itself. The advantages of representing aerosols by their lower-order moments have been discussed by McGraw *et al.* [1995, 1998], McGraw [1997], and Barrett and Webb [1998]. Simulations of aerosol dynamics based on moments are free from the problems associated with numerical diffusion (in size space) and tend to have greatly superior computational speed when compared with the sectional approach [Frenklach and Harris, 1987]. Moment-based approaches initially suffered from the limitation of either being restricted to very special condensation/coagulation kernels, or the necessity of assuming certain functional forms for the particle size distribution in order to

obtain a closed set of moment evolution equations. However, with the introduction of quadrature techniques [McGraw, 1997; Barrett and Webb, 1998], condensation/coagulation kernels of arbitrary functional form can be treated without the need for *a priori* assumptions regarding the form of the particle size distribution, and size-dependent kernels for removal processes and cloud activation are also easily handled. Thus the method of moments has become a viable candidate for modeling aerosols under very general conditions. In parallel to these dynamical developments, a number of studies have established powerful tools for predicting aerosol physical and optical properties directly from these lower-order moments [McGraw *et al.*, 1995; McGraw, 1997; Yue *et al.*, 1997; Wright, 2000].

In this letter we present results from incorporation of the QMOM in the three-dimensional chemical transport and transformation model (GChM-O) of Benkovitz *et al.* [1994]. The QMOM-based aerosol microphysical module presently tracks the six lowest-order radial moments for three externally-mixed aerosol populations: a sulfate aerosol, a sea salt aerosol, and a bimodal continental background aerosol, as well as other microphysical quantities. Optical properties are computed during post-processing of the simulated moments using the Multiple Isomomental Distribution Aerosol Surrogate (MIDAS) approach [Wright, 2000], and we include in this report a calculation of the geographic distribution of the clear-sky (direct) forcing of the sulfate aerosol to illustrate some of the end-result capabilities of the moment-based approach.

2. Model Description

Here we present a brief overview of the model. A more complete description will follow in a full article in preparation for the *Journal of Geophysical Research*. The Global Chemistry Model driven by Observation-derived meteorological data (GChM-O) [Benkovitz *et al.*, 1994; Benkovitz and Schwartz, 1997] is a 3-D Eulerian transport and transformation model which was developed to simulate mass loadings of tropospheric sulfate. It represents emissions of anthropogenic SO₂, sulfate and biogenic sulfur species, horizontal and vertical transport, vertical turbulent mixing, gas-phase oxidation of SO₂ and dimethylsulfide, aqueous phase oxidation of SO₂, and wet and dry deposition of SO₂, sulfate and methanesulfonic acid. The meteorological driver is the 6-hour output from the forecast model of the European Centre for Medium-Range Weather Forecasts (ECMWF). The horizontal resolution is 1.125°, and there are 15 vertical levels extending to about 100 hPa. Clouds in the model provide an environment for aqueous chemical reactions, provide wet removal, and in the case of convective clouds, supply mixing and subgrid-scale vertical motions. A stratiform or convective cloud module is activated according to the ECMWF meteorological fields. Details can be found in Benkovitz [1994].

Copyright 2000 by the American Geophysical Union.

Paper number 1999GL010975.
0094-8276/00/1999GL010975\$05.00

2.1. The Quadrature Method of Moments (QMOM)

For a size distribution $f(r)$ of spherical particles of radius r the k^{th} radial moment is defined as

$$\mu_k = \int_0^{\infty} r^k f(r) dr .$$

The QMOM employs only the low-order moments (six moments here, $k = 0-5$) to model aerosol populations and properties. The particle size distribution is not explicitly modeled, nor is a functional form assumed for the size distribution. An N -point quadrature yields an approximate (and often very good) evaluation of integrals of the form

$$I = \int_0^{\infty} \sigma(r) f(r) dr \quad \text{or} \quad I = \int_0^{\infty} \int_0^{\infty} \sigma(r_1, r_2) f(r_1) f(r_2) dr_1 dr_2$$

from knowledge of the first $2N$ moments for any kernel functions $\sigma(r)$ or $\sigma(r_1, r_2)$. The approximation is most accurate with smooth kernels, such as condensation and coagulation kernels, and errors are typically well under 1% for these processes over significant aerosol evolution. The approximation is exact for kernels of polynomial form provided the degree of the polynomial does not exceed $2N-1$. The QMOM dynamics is exact for free-molecular condensational growth, and for the even-order moments under diffusion-controlled growth. The quadrature approach can accommodate kernels of arbitrary functional form for condensation, coagulation, dry deposition, wet removal, cloud activation and other size-dependent processes without assuming a functional form for the particle size distribution. The N quadrature abscissas and weights $\{r_i, w_i\}$ are readily obtained from the lower $2N$ moments via the subroutine ORTHOG [Press et al., 1992].

2.2. Multiple Isomomental Distribution Aerosol Surrogate (MIDAS) Technique

Aerosol optical properties and radiative influence are computed from the six moments at each grid cell using the MIDAS technique. This technique (currently used for post-processing only) computes desired quantities using families of smooth multimodal distributions composed of lognormals or modified gammas, each distribution consistent with the set of modeled moments. Evaluation of this technique for 28 test distributions derived from field observations of marine, continental, urban and stratospheric aerosols yielded an average magnitude of error less than 2% for several optical properties. For the single-wavelength shortwave forcing results presented here, the average magnitude of error is expected to be less than 1% [Wright, 2000]. These errors, which show no systematic bias (positive and negative deviations occur with equal frequency) arise from the fact that the optical properties are determined from six moments rather than the size distribution itself. Errors of this magnitude are small compared to the uncertainties in both large-scale modeling and present knowledge of the atmospheric aerosol.

2.3. Aerosol Populations

The model currently represents an external mixture of three aerosol populations: sulfate aerosol, sea salt aerosol, and a bimodal continental background aerosol. In addition to its six lowest-order radial moments, all populations other than the sulfate aerosol are also characterized by the sulfate mass per particle. Each aerosol type undergoes transport, vertical-turbulent and convective cloud mixing, size-resolved dry deposition, and wet removal. To prevent the numerical approximations in the transport algorithm from yielding unphysical moment sets, only the number moment (μ_0) of

each population is explicitly transported (or mixed), and explicit inter-cell fluxes of μ_0 are used to evolve the higher moments in each cell due to advection. This corresponds to the transport and mixing of a vector (rather than a scalar) quantity whose elements (the normalized moments) represent internal coordinates of the aerosol. The several aerosol populations are coupled through competition for $\text{H}_2\text{SO}_4(\text{g})$ and through scavenging of the sulfate aerosol via coagulation with the other populations. The scavenging routine is called whenever both the sulfate and scavenging populations have coexisting number concentrations exceeding preset threshold values.

2.4. Sulfate Aerosol

This population has two sources: primary particulate emissions and new particle formation via binary $\text{H}_2\text{SO}_4\text{-H}_2\text{O}$ nucleation. Primary emissions for the moments are derived from lognormal distributions [Whitby, 1978] with the normalization determined by the sulfate mass emission rate for each location. For nucleation, the Jaecker-Voirol Mirabel expression, as parameterized in Fitzgerald et al. [1998a], is used without any 'tuning' prefactor, as none was needed to obtain copious new particle production. After transport and mixing of the dry aerosol, and before condensational growth and coagulation are performed, the moments are converted to their ambient values according to the local RH using the water uptake data of Tang and Munkelwitz [1994]. With the assumption of a size-independent water uptake ratio $\beta = r_{\text{wet}}/r_{\text{dry}}$, the k^{th} moment scales as $\mu_k(\text{wet}) = \beta^k \mu_k(\text{dry})$ when the dry aerosol equilibrates with water. Using the quadrature weights and abscissas, the sulfate aerosol is allowed to undergo a size-resolved cloud activation resulting in variable numbers of cloud condensation nuclei (CCN) and a variable activated fraction of the aerosol number concentration. In the absence of a more detailed cloud module in GChM-O, cloud processing is performed by assuming a maximum supersaturation for each cloud type, from which the minimum dry radius required for cloud drop activation is computed using the Kohler equation. All abscissas ("particle sizes") greater than this minimum radius are then taken as CCN. Once the total number of CCN is determined, the total sulfate mass produced by aqueous chemistry during the time step (as already determined by the chemistry module) is divided equally among all CCN. The moments are then recomputed using the updated abscissas. There is no feedback to supersaturation in this simplified model, and thus the number of activated drops equals the number of CCN. The cloud droplet spectrum, droplet coalescence, and the indirect effect are not treated within the present model.

2.5. Sea Salt Aerosol

This population was represented primarily because its surface area density could provide a significant sink for H_2SO_4 . The production rate for moments of the sea salt size distribution is derived by integrating over the size-resolved fluxes given in Smith et al. [1993]; the resultant aerosol undergoes water uptake and loss with RH in like manner to the sulfate aerosol. Condensational growth from H_2SO_4 is not enabled, as it is very small relative to the size of these super-micron particles. In the calculations reported here, the loss of $\text{H}_2\text{SO}_4(\text{g})$ to sea salt is significant at certain locations and times; however, coagulation scavenging of sulfate aerosol particles is insignificant. All sea salt particles are treated as being sufficiently large to serve as CCN.

2.6. Continental Background Aerosol

This population was introduced to represent the total (non-sulfate aerosol) surface area density produced over the continents, as pre-existing surface area plays a large role in governing the formation of new particles. The two modes (represented by 12 moments and 2 sulfate mass variables total) are given surface source rates constant in space and time, with the moments of sources derived from assumed lognormal distributions. The source rates were adjusted to yield reasonable background surface areas. Condensational growth due to H_2SO_4 is not enabled in view of the crude nature of the source term, but the sulfate mass is explicitly tracked in the model. Coagulation scavenging of sulfate particles is enabled but is insignificant in the present calculations. These particles do not serve as CCN in these simulations.

3. Results

The simulated period began October 1, 1986, with no aerosol initially present in the model domain, which extends from 140.6°W to 61.9°E and 12.4°N to 81.0°N . Previous work with GChM-O tracking sulfate mass only indicated that a period of ~ 14 days is sufficient for independence of initial conditions in the model domain, although this requires further investigation regarding the aerosol microphysics. No aerosol boundary fluxes were included in the present simulation, and Figure 1 presents only that aerosol emitted or generated within the model domain during the simulated month. For illustrative purposes we display results only for the sulfate aerosol. All results in Figure 1 are for October 22, 1986, 0600 UT.

Figure 1(a) presents the modeled sulfate aerosol number concentration at the lowest model level, centered approximately 32 meters above the surface. Over the North Atlantic and remote continental regions modeled values are typically $\sim 10^3 \text{ cm}^{-3}$, whereas continental regions with greater anthropogenic influence may show number concentrations a few times 10^4 cm^{-3} ($44,000 \text{ cm}^{-3}$ is the maximum in this figure). So far we have detected very little new particle formation in the marine boundary layer with the (unscaled) Jaeger-Voirol Mirabel nucleation rate, consistent with the results of Fitzgerald *et al.* [1998b]. The large concentrations of small particles over Greenland may be the result of low temperatures enhancing the nucleation rate.

Figures 1(b, c) present the modeled sulfate aerosol number mean radius ($\bar{r} = \mu_1/\mu_0$) and effective radius ($r_{\text{eff}} = \mu_3/\mu_2$) at the lowest model level. For a monodisperse distribution, $r_{\text{eff}} = \bar{r}$; the extent to which r_{eff} exceeds \bar{r} is an indication of the breadth of the underlying (but unknown) particle size distribution. A qualitative measure of the width of the underlying distribution is evaluated offline as $\sigma_g = \exp\{\{\ln(r_{\text{eff}}/\bar{r})\}^2\}^{1/2}$; for a lognormal distribution this would yield the geometric standard deviation. For the values of r_{eff} and \bar{r} in these figures, σ_g ranges from 1.25 to 4.30. By comparison, a monodisperse distribution has $\sigma_g = 1$, typical nuclei and accumulation modes have $\sigma_g \approx 1.7$ and 2.0, respectively [Whitby, 1978], and very broad multimodal distributions including particles of radii 10^{-3} to $10^2 \mu\text{m}$ have been represented using $\sigma_g = 6$ [Vasconcelos *et al.*, 1998].

Figures 1(d) and 1(e) show column integrals of the dry and ambient condensed sulfate aerosol volumes, respectively. As the model treats sulfate as ammonium sulfate, multiplication of the values in Figure 1(d) by $[1.77 \text{ g } (\text{NH}_4)_2\text{SO}_4 \text{ cm}^{-3}]/[96 \text{ g sulfate}/132 \text{ g } (\text{NH}_4)_2\text{SO}_4]$ yields the column mass loading in grams sulfate m^{-2} .

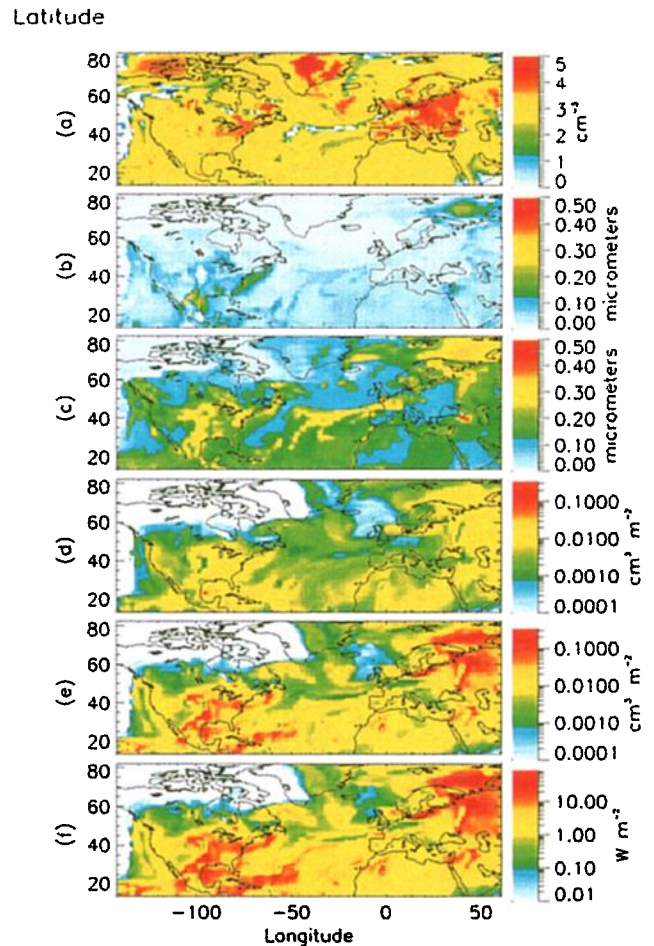


Figure 1. Modeled sulfate aerosol on October 22, 1986, 0600 UT. (a) \log_{10} number concentration (μ_0) at $z = 32$ meters, (b) number mean radius ($\bar{r} = \mu_1/\mu_0$) at $z = 32$ meters, (c) effective radius ($r_{\text{eff}} = \mu_3/\mu_2$) at $z = 32$ meters, (d) column integral of condensed aerosol volume for the dry aerosol, (e) column integral of condensed aerosol volume for the ambient aerosol, and (f) magnitude of the clear-sky forcing (ΔF) at a wavelength of 550 nm. White regions indicate values below the plotting scale.

Figure 1(f) presents the clear-sky radiative forcing of the sulfate aerosol, estimated following Charlson *et al.* [1992]. (In this calculation the wavelength was taken as 550 nm and the refractive index was taken as $1.4 - 0i$, independent of relative humidity). The forcing involves an integral over the size distribution $f(r, z)$, as well as over the vertical coordinate z :

$$\Delta F = -\frac{1}{2} F_T T^2 (1 - R_s)^2 \left[\pi \int r^2 Q(r) \beta_U(r, \theta_0) f(r, z) dr \right] dz$$

F_T is the solar constant (1368 W/m^2), T the Rayleigh transmittance (0.76), R_s the surface albedo (0.15 land, 0.05 ocean), $Q(r)$ the Mie scattering efficiency, $\beta_U(r, \theta_0)$ the upscatter fraction, and θ_0 the solar zenith angle, here assigned a constant value of 60° . The factor of 1/2 in this expression, which derives from the fact that only half of the Earth is illuminated at a given time, yields a forcing that can be compared to long-term average forcing. In the present calculations, MIDAS is used for each grid cell to compute the integral in square brackets from the moments of the size distribution at ambient relative humidity; this integral, when multiplied by the geophysical factors, yields the contribution to the forcing for each cell.

We comment on several features in Figure 1(f). Strong spatial variation of forcing is observed, as expected from the mass loading, which itself is highly variable in both space and time. The forcing exhibits much better spatial correlation with ambient volume than with dry volume, demonstrating the importance of explicitly representing RH-dependent growth as well as particle dry size in models. Peak values in the clear-sky forcing are about -80 W/m^2 and thus may present a substantial local perturbation of climate. The two peak values of forcing in the domain (both in the Gulf of Mexico) were -81.5 and -79.8 W/m^2 ; some associated parameters are, for each location, respectively: sulfate mass burden, 0.0569 and $0.105 \text{ gSO}_4^{-2}/\text{m}^2$; relative humidity, 92 and 84% ; water uptake ratio, 1.87 and 1.55 ; normalized forcing, -1430 and $-763 \text{ W/gSO}_4^{-2}$. These values of normalized forcing are consistent with Nemesure *et al.* [1995]. The use of a constant refractive index, corresponding to 80% RH, slightly overestimates normalized forcing for $\text{RH} > 80\%$, but this does not result in significant enhancement of these forcing values. For instantaneous forcing the $1/2$ factor would be removed, yielding forcings of twice the magnitude shown in Figure 1(f). The domain average of the plotted clear-sky forcing is -3.6 W/m^2 ; with the assumption of a climatological average cloud cover of $A_c = 0.6$ that value is derated by the factor $(1-A_c)$ to -1.4 W/m^2 . Such a value is comparable to values of -0.2 to -1.6 W/m^2 cited by Bergstrom and Russell [1999] for the annual average forcing by sulfate aerosol in the Northern hemisphere.

4. Conclusions

One of the advantages of moment methods is their modest computational and storage requirements; in the present model each aerosol population is represented with only six or seven parameters (6 moments and sulfate mass per particle for the non-sulfate populations). The pilot one-month simulation reported here required 58.9 CPU hours on a Sun Spark Ultra-Enterprise.

We note also that the QMOM easily generalizes to the case of bivariate distribution functions, as would be used to represent, for example, populations of non-spherical particles [Tandon and Rosner, 1999]. Bivariate moment methods will be the subject of a forthcoming report.

In conclusion, these results demonstrate the capability of moment techniques, in particular the QMOM and MIDAS, to represent aerosol dynamical processes including particle nucleation, condensation/evaporation, coagulation, dry deposition, wet removal, cloud droplet activation, and transport processes in complex 3-D Eulerian models, and to yield aerosol optical properties from the modeled moments. Accordingly, the methods illustrated here can provide a valuable new approach to modeling aerosol dynamics, properties, and radiative influence.

Acknowledgments. This research was supported in part by NASA through interagency agreement number W-18,429 as part of its interdisciplinary research program on tropospheric aerosols, and in part by the Environmental Sciences Division of the U.S. Department of Energy (DOE) as part of the Atmospheric Chemistry Program, and was performed under the auspices of DOE under Contract No. DE-AC02-98CH10886.

References

- Barrett, J. C., and N. A. Webb, A comparison of some approximate methods for solving the aerosol general dynamic equation, *J. Aerosol Sci.*, **29**, 31-39, 1998.
- Benkovitz, C. M., C. M. Berkowitz, R. C. Easter, S. Nemesure, R. Wagener, and S. E. Schwartz, Sulfate over the North Atlantic and adjacent continental regions: Evaluation for October and November 1986 using a three-dimensional model driven by observation-derived meteorology, *J. Geophys. Res.*, **99**, 20,725-20,756, 1994.
- Benkovitz, C. M., and S. E. Schwartz, Evaluation of modeled sulfate and SO_2 over North America and Europe for four seasonal months in 1986-1987, *J. Geophys. Res.*, **102**, 25,305-25,338, 1997.
- Bergstrom, R. W., and P. B. Russell, Estimation of aerosol direct radiative effects over the mid-latitude North Atlantic from satellite and in situ measurements, *Geophys. Res. Lett.*, **26**, 1731-1734, 1999.
- Charlson, R. J., S. E. Schwartz, J. M. Hales, R. D. Cess, J. A. Coakley, J. E. Hansen, and D. J. Hofmann, Climate forcing by anthropogenic aerosols, *Science*, **255**, 423-430, 1992.
- Fitzgerald, J. W., W. A. Hoppel, and F. Gelbard, A one-dimensional sectional model to simulate multicomponent aerosol dynamics in the marine boundary layer. I. Model description, *J. Geophys. Res.*, **103**, 16,085-16,102, 1998a.
- Fitzgerald, J. W., J. J. Marti, W. A. Hoppel, G. M. Frick, and F. Gelbard, A one-dimensional sectional model to simulate multicomponent aerosol dynamics in the marine boundary layer, II. Model application, *J. Geophys. Res.*, **103**, 16,103-16,117, 1998b.
- Frenklach, M. and S. J. Harris, Aerosol dynamics modeling using the method of moments, *J. Coll. Interface Sci.*, **118**, 252-261, 1987.
- Haywood, J. M., V. Ramaswamy, and B. J. Soden, Tropospheric Aerosol Climate Forcing in Clear-Sky Satellite Observations over the Oceans, *Science*, **283**, 1299-1303, 1999.
- McGraw, R., Description of aerosol dynamics by the quadrature method of moments, *Aerosol Sci. Technol.*, **27**, 255-265, 1997.
- McGraw, R., P. I. Huang, and S. E. Schwartz, Optical properties of atmospheric aerosols from moments of the particle size distribution, *Geophys. Res. Lett.*, **22**, 2929-2932, 1995.
- McGraw, R., S. Nemesure, and S. E. Schwartz, Properties and evolution of aerosols with size distributions having identical moments, *J. Aerosol Sci.*, **29**, 761-772, 1998.
- Press, W. H., S. A. Teukolsky, W. T. Vetterling, and B. P. Flannery, *Numerical Recipes in FORTRAN*, Cambridge University Press, Cambridge, 1992.
- Smith, M. H., P. M. Park, and I. E. Consterdine, Marine aerosol concentrations and estimated fluxes over the sea, *Quart. J. Royal Meteor. Soc.*, **119**, 809-824, 1993.
- Tandon, P., and D. E. Rosner, Monte Carlo simulation of particle aggregation and simultaneous restructuring, *J. Colloid Interface Sci.*, **213** (2), 273-286, 1999.
- Tang, I. N., and H. R. Munkelwitz, Water activities, densities, and refractive indices of aqueous sulfates and sodium nitrate droplets of atmospheric importance, *J. Geophys. Res.*, **99**, 18,801-18,808, 1994.
- Vasconcelos, L. A. de P., E. S. Macias, and W. H. White, On the relationship of aerosol optics to moments of particle size distribution, *Geophys. Res. Lett.*, **25**, 4189-4192, 1998.
- Whitby, K., The physical characteristics of sulfur aerosols, *Atmos. Environ.*, **12**, 125-159, 1978.
- Wright, D. L., Retrieval of optical properties of atmospheric aerosols from moments of the particle size distribution, *J. Aerosol Sci.*, **31**, 1-18, 2000.
- Yue, G. K., J. Lu, V. A. Mohnen, P.-H. Wang, V. K. Saxena, and J. Anderson, Retrieving aerosol optical properties from moments of the particle size distribution, *Geophys. Res. Lett.*, **24**, 651-654, 1997.

C. M. Benkovitz, R. McGraw, S. E. Schwartz, and D. L. Wright, Environmental Chemistry Division, Department of Applied Science, Brookhaven National Laboratory, Upton, NY 11973-5000.

(Received August 6, 1999; revised September 28, 1999; accepted January 5, 2000.)